THERMAL ANALYSIS OF GENERATORS

Erol Kurt

Gazi University, Technology Faculty, Dep. Electrical & Electronics Engineering, Ankara, Turkey

ekurt52tr@yahoo.com

Cooling and Heat Transfer

1 Importance of Thermal Analysis

During the operation of an electrical machine, heat is generated due to power losses in electric and magnetic circuits and mechanical (rotational) losses. To ensure a long operational life for the machine, these losses must be removed as far as possible from the machine so that the temperature limitations established for the machine materials, such as insulating materials, lubricants and PMs are complied with. In addition to the consideration of the machine's operational life, a lower operating temperature reduces extra winding losses introduced by the temperature coefficient of the electric resistance — eqn (3.47).

Whereas extensive research has been devoted to the thermal studies of conventional electrical machines, AFPM machines have received very little attention [128, 245, 260]. Owing to the fact that AFPM machines possess a relatively large air gap volume and quite often have multi-gaps, the general perception is that AFPM machines have better ventilation capacity than their radial field counterparts [52, 106].

Since the external diameter increases rather slowly with the increase of output power, i.e. $D_{out} \propto \sqrt[3]{P_{out}}$ the existing heat dissipation capacity may be insufficient to cope with excessive heat at certain power ratings, so that more effective means of cooling have to be enforced. Thus, quantitative studies of the heat dissipation potential of AFPM machines with vastly different topologies is important.

2 Heat Transfer Modes

Heat transfer is a complex phenomenon presenting formidable analytical difficulties. Heat is removed from an electrical machine by a combination of *conduction*, *radiation* and *convection* processes to the ambient air and surroundings.

1 Conduction

When a temperature gradient exists in a solid body, such as in the copper, steel, PMs or the insulation of an electrical machine, heat is transferred from the high-temperature region of temperature ϑ_{hot} to the low-temperature region of temperature ϑ_{cold} according to *Fourier's law*, which is given as:

$$\Delta P_c = -kA\frac{\partial \vartheta}{\partial x} = \frac{kA}{l}\left(\vartheta_{hot} - \vartheta_{cold}\right) \qquad 1)$$

where ΔP_c is the rate of heat conduction, A is the area of the flow path, l is the length of the flow path and k is the thermal conductivity of the material. The latter is experimentally determined and is relatively insensitive to temperature changes. Thermal properties of typical materials used for AFPM machines are given in Table 8.1, where c_p is the specific heat of material at constant pressure.

Table 1. Selected thermal properties of materials

Material (20°C)	Grade	ρ kg/m^3	c_p J/(kg °C)	k W/(m °C)
Air	-	1.177	1005	0.0267
Water	-	1000	4184	0.63
Mica	-	3000	813	0.33
Epoxy resin	-	1400	1700	0.5
Copper	-	8950	380	360
Aluminum	Pure	2700	903	237
	Alloy (cast)	2790	883	168
Steel	1% Carbon	7850	450	52
	Silicon	7700	490	20-30
Permanent magnet	Sintered NdFeB	7600 to 7700	420	9

2 Radiation

The net *radiant energy* interchange between two surfaces with a temperature difference is a function of the absolute temperature, the emissivity and the geometry of each surface. If heat is transferred by radiation between two gray surfaces of finite size, A_1 and A_2, and temperature, ϑ_1 and ϑ_2 (in Celsius degree), the rate of heat transfer, ΔP_r, may be written as

$$\Delta P_r = \sigma \frac{(\vartheta_1 + 273)^4 - (\vartheta_2 + 273)^4}{\frac{1-\varepsilon_1}{\varepsilon_1 A_1} + \frac{1}{A_1 F_{12}} + \frac{1-\varepsilon_2}{\varepsilon_2 A_2}} \qquad 2)$$

where σ is the *Stefan-Boltzmann* constant, F_{12} is the shape factor which takes into account the relative orientation of the two surfaces and ε_1 and ε_2 are their respective emissivities which depend on the surfaces and their treatment. An ideal surface or body that absorbs and emits energy at maximum rate is called *black surface* or *body*. Real surfaces or bodies are normally approximated as gray surfaces or bodies where $0 < \varepsilon < 1$. Some selected emissivities related to AFPM machines are given in Table 2.

Table 2. Selected emissivities relevant to AFPM machines

Material	Surface condition	Emissivity, ε
Copper	Polished	0.025
Epoxy	Black	0.87
	White	0.85
Mild steel	-	0.2-0.3
Cast iron	Oxidized	0.57
Stainless steel	-	0.2-0.7
Permanent magnet, NdFeB	Uncoated	0.9

3 Convection

Convection is the term describing heat transfer from a surface to a moving fluid. The rate of convective heat transfer, ΔP_v, is given according to *Newton's law of cooling* as:

$$\Delta P_v = hA(\vartheta_{hot} - \vartheta_{cold})$$

where h is the convection heat transfer coefficient, which is a rather complex function of the surface finish and orientation, fluid properties, velocity and temperature, and is usually experimentally determined. The coefficient h increases with the velocity of the cooling medium relative to the cooled surface. For a surface with forced ventilation, the following empirical relation may be used [159], i.e.

$$h_f = h_n(1 + c_h\sqrt{v})$$

where h_f and h_n are the coefficients of heat transfer for the forced and natural convection respectively, v is the linear velocity of cooling medium and $c_h \approx 0.5$ to 1.3 is an empirical coefficient.

Some important formulae for evaluating convective heat transfer coefficients of AFPM machines are discussed in the following sections.

Convection Heat Transfer in Disc Systems

The rotating disc system plays a major role in the cooling and ventilation of the AFPM machine. Accurately determining the convection heat transfer coefficients needs thorough theoretical and experimental investigation because of the complexity of flow regimes.

In this section the convection heat transfer coefficients in different parts of the AFPM machine are evaluated, exploiting a number of existing models.

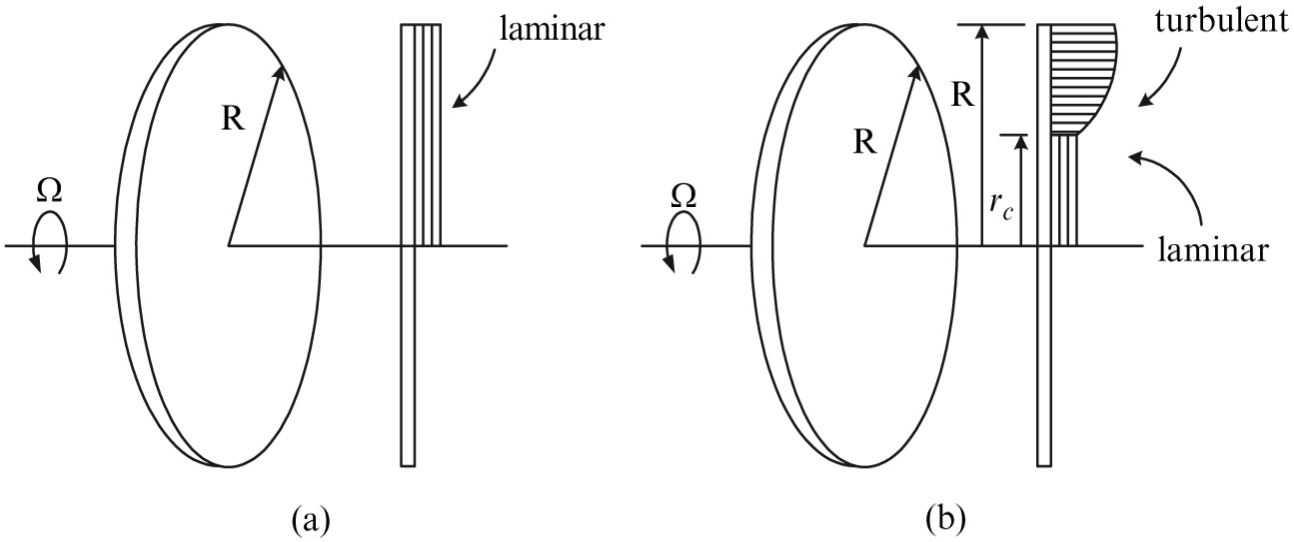

Fig. 1. Free rotating disc: (a) in laminar flow, (b) transition from laminar to turbulent flow.

Free rotating disc

The average heat transfer coefficient at the outside surface of a rotating disc may be evaluated using the formula developed for a free rotating disc , i.e.

$$\bar{h} = \frac{k}{R}\overline{Nu} \qquad .5)$$

where R is the radius of the disc and the average Nusselt number $\overline{Nu}$ is given according to the different flow conditions as follows:

(i) For combined effects of free convection and rotation in laminar flow

$$\overline{Nu} = \frac{2}{5}(Re^2 + Gr)^{\frac{1}{4}} \qquad .6)$$

$$G_r = \frac{\beta g R^3 \pi^{3/2} \Delta\vartheta}{\nu^2} \qquad 7)$$

where Re is the Reynolds number according to eqn (2.72), β is the coefficient of thermal expansion, ν is the kinematic viscosity of the fluid (m^2/s) and $\Delta\vartheta$

is the temperature difference between the disc surface and surrounding air.

(ii) For a combination of laminar and turbulent flow with the transition at a radius r_c

$$\overline{Nu} = 0.015 Re^{\frac{4}{5}} - 100(\frac{r_c}{R})^2 \qquad 8)$$

where

$$r_c = (2.5 \times 10^5 \nu/\Omega)^{1/2} \qquad 9)$$

The angular speed $\Omega = 2\pi n$ when n is the rotational speed in rev/s. It is instructive to compare the heat transfer capabilities between a rotation disc and a stationary disc. If we consider a steel disc, which has a diameter of 0.4 m and rotates at 1260 rpm., the convection heat transfer coefficient may be calculated as 41 W/(m^2 $^\circ$C), which is about ten times that of the same disc at standstill. Alternatively, one can say that the effective heat dissipation area of the same disc can be increased by a factor of 10 when the disc rotates at the specific speed.

Rotor radial peripheral edge

The heat transfer correlations for the radial periphery of the rotor disc are similar to those of a rotating cylinder in air. In this case the average heat transfer coefficient is given as

$$\bar{h}_p = (k/D_{out})\overline{Nu} \qquad 10)$$

where D_{out} is the outer diameter of the rotor disc, the average Nusselt number is given by

$$\overline{Nu} = 0.133\ Re_D^{2/3} Pr^{1/3} \qquad .11)$$

and Reynolds number at the disc periphery is

$$Re_D = \Omega D_{out}^2/\nu \qquad 12)$$

Note that a uniform temperature distribution in the cylinder is normally assumed when eqn (8.10) is used. Since $\bar{h}_p$ is proportional to the angular speed Ω, it may be concluded that the rotor periphery plays an increasingly important role in the heat dissipation as Ω increases.

Rotor-stator system

As seen in Fig. 8.2, an AFPM machine consists of a number of rotating and stationary discs. The heat transfer relations between a rotating and a stationary disc are of paramount importance in the thermal calculations. Due

to centrifugal effects, there is a forced flow between the two discs, which increases the local heat transfer rate compared with that of a free disc. The relative increase will depend on the gap ratio, $G = g/R$, where g is the clearance between the rotor and the stator and R is the radius of the disc, the mass flow rate and the rotational speed of the system

Having radial channels and thick impellers, an air-cooled AFPM machine may be regarded as a poorly designed fan from a fluid flow perspective. Its tangential velocity component is much larger than the radial component. Thus, the heat transfer rate near the rotating disc shows more dependence on the rotational Reynolds number, Re_r .

Owen provided an approximate solution for the flow between a rotating and a stationary disc, which relates the average Nusselt number to the moment coefficient of the stator-side rotor face, C_{mo}, by the following equation:

$$\begin{cases} \overline{Nu} = Re_r C_{mo}/\pi \\ \\ C_{mo} Re_r^{1/5} = 0.333 \lambda_T \end{cases} \quad (13)$$

where λ_T is a *turbulence parameter* given as a function of volumetric flow rate, Q, as follows

$$\lambda_T = \frac{Q}{\nu R} Re_r^{-\frac{4}{5}} \qquad 14)$$

By replacing λ_T in eqn (8.13) with eqn 14), the average Nusselt number becomes

$$\overline{Nu} = 0.333 \ \frac{Q}{\pi \nu R} \qquad 15)$$

As discussed in [208], it has been shown that for a small gap ratio ($G < 0.1$) the flow in the air-gap space between the rotor and stator can be treated as a boundary layer. Whilst it is not absolutely true that the convective heat transfer coefficient from the stator to the air flow is close to that of the air flow to a rotating disc, the same heat transfer coefficient may be assumed in the thermal circuit simulation.

3 Cooling of AFPM Machines

Depending on the size of the machine and the type of enclosures, different arrangements for cooling may be used. From a cooling perspective, AFPM machines may be classified into two categories as follows:

- *machines with self-ventilation*, in which cooling air is generated by a rotating disc, PM channels or other fan-alike devices incorporated with the rotating part of the machine, and

- *machines with external ventilation*, in which the cooling medium is circulated with the aid of external devices, for an example, a fan or a pump.

3.1 AFPM Machines With Self-Ventilation

The majority of AFPM machines are air-cooled. Compared with conventional electrical machines, a particularly advantageous feature of disc-type AFPM machines from a cooling perspective is that they possess inherent self-ventilation capability. Fig. 8.2 shows the layout and active components of a typical AFPM machine. A close examination of the machine structure reveals that an air stream will be drawn through the air inlet holes into the machine and then forced outwards into the radial channel as the rotor discs rotate. The PMs in fact act as impeller blades. The fluid behaviour of the AFPM machine is much like that of a centrifugal fan or compressor.

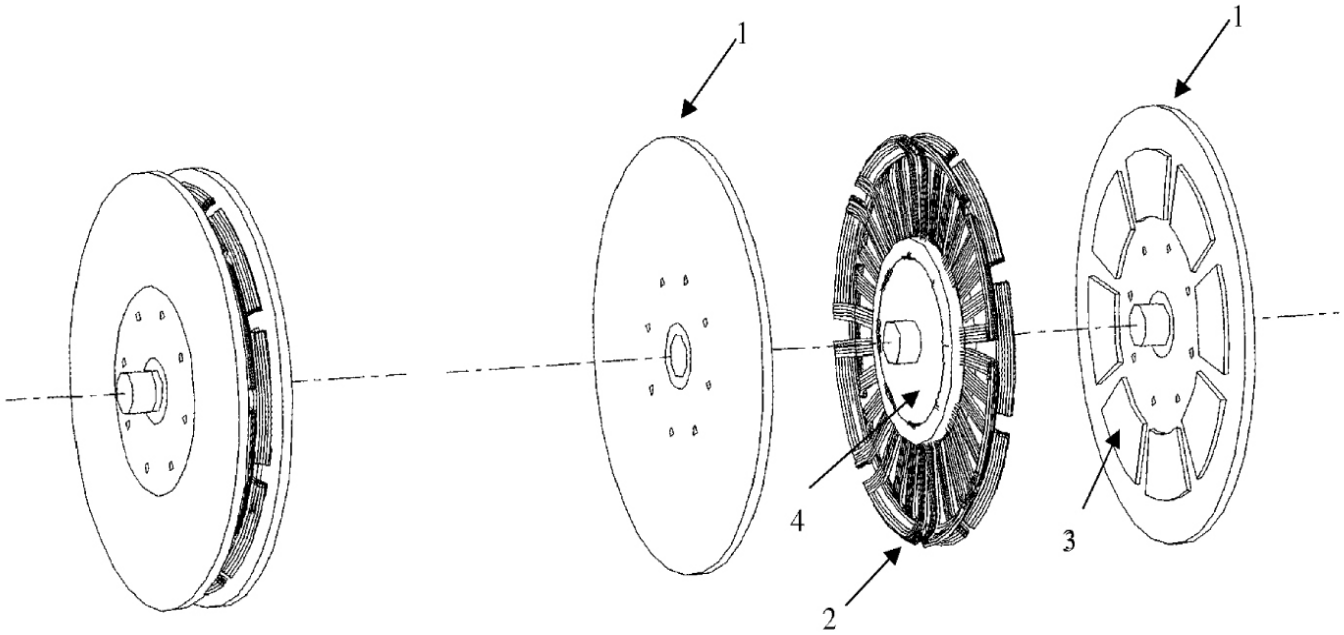

Fig. 2. Exploded view of an AFPM machine: 1 — rotor disc, 2 — stator winding, 3 — PM, and 4 — epoxy core.

The Ideal Radial Channel

According to the theory of an ideal impeller, a number of assumptions have to be made to establish the one-dimensional model of the ideal radial channel

(a) there are no tangential components in the flow through the channel;
(b) the velocity variation across the width or depth of the channel is zero;
(c) the inlet flow is radial, which means that air enters the impeller without pre-whirl;

(d) the pressure across the blades can be replaced by tangential forces acting on the fluid;
(e) the flow is treated as incompressible and frictionless.

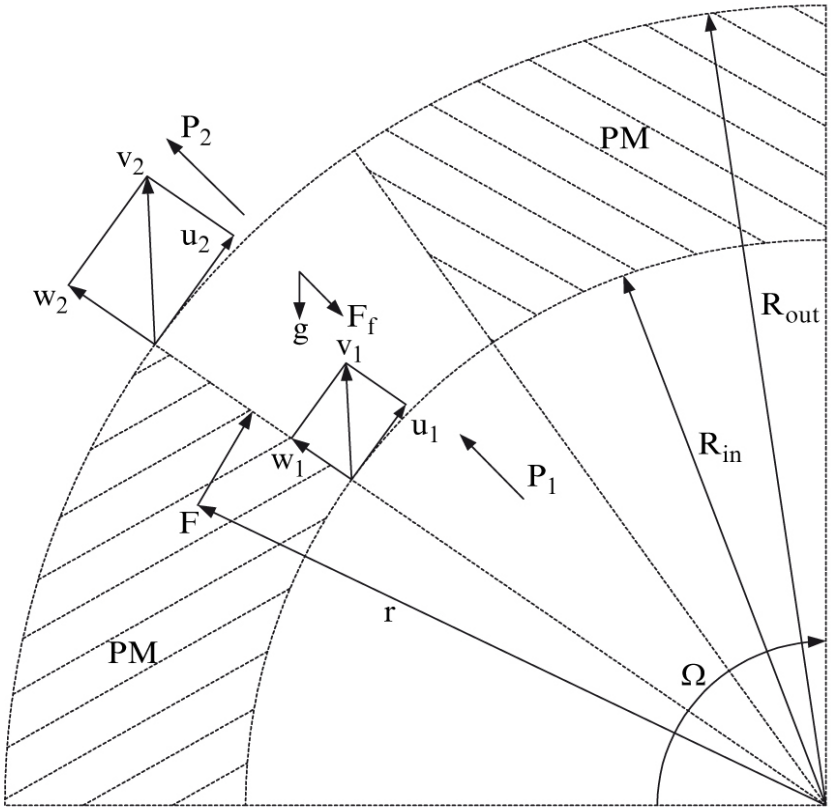

Fig. 3. Velocity triangles for a PM channel.

Figure 3 shows a radial channel with the velocity triangles drawn at the inlet and the outlet. It can be observed that the pressures at the inlet p_1 and the outlet p_2, and friction F_{fr} make no contribution to the sum of the momentum, $\sum M_0$. If gravity is ignored, the general representation of conservation of momentum takes the following form

$$\sum M_0 = \frac{\partial}{\partial t}[\int_{cv} (\mathbf{r} \times \mathbf{v})\rho dV] + \int_{cs} (\mathbf{r} \times \mathbf{v})\rho(\mathbf{v} \cdot \mathbf{n})dA \qquad 16)$$

where $\mathbf{r}$ is the position vector from 0 to the elemental control volume dV and $\mathbf{v}$ is the velocity of the element.

For steady-state, one-dimensional air flowing between the entrance and exit of the channel, eqn .16) may be simplified as:

$$\sum M_0 = T_0 = (\mathbf{R}_{out} \times \mathbf{u_2})\dot{m}_2 - (\mathbf{R}_{in} \times \mathbf{u_1})\dot{m}_1 \qquad 17)$$

where $\dot{m}_2 = \dot{m}_1 = \rho Q$, $u_1 = \Omega R_{in}$ and $u_2 = \Omega R_{out}$. The input shaft power P_{in} is then given by:

$$P_{in} = T_0 \Omega = \rho Q \Omega^2 (R_{out}^2 - R_{in}^2) \quad 18)$$

Re-arranging the above equation gives:

$$\frac{P_{in}}{Q} = \rho \Omega^2 (R_{out}^2 - R_{in}^2) \quad 19)$$

Based on the principle of conservation of energy, the input shaft power may be given as:

$$P_{in} = \dot{m}(\frac{p_2 - p_1}{\rho} + \frac{w_2^2 - w_1^2}{2} + z_2 - z_1 + U_2 - U_1) \quad 20)$$

If the potential $(z_2 - z_1)$ and internal energy $(U_2 - U_1)$ (friction) are ignored, eqn .20) may be written in the same units as eqn .19) as:

$$\frac{P_{in}}{Q} = (p_2 - p_1) + \rho\frac{w_2^2 - w_1^2}{2} \qquad 21)$$

If equations 19) and .21) are equated and noting that $w_1 = Q/A_1$ and $w_2 = Q/A_2$, where A_1 and A_2 are the cross-section areas of the inlet and outlet of the channel respectively, the pressure difference Δp between the entrance and exit of the radial channel (shown in Fig. 3) may be expressed as:

$$\Delta p = p_2 - p_1 = \rho\Omega^2(R_{out}^2 - R_{in}^2) - \frac{\rho}{2}(\frac{1}{A_2^2} - \frac{1}{A_1^2})Q^2 \qquad 22)$$

Eqn (22) may be termed the *ideal equation* describing the air flow through the radial channel.

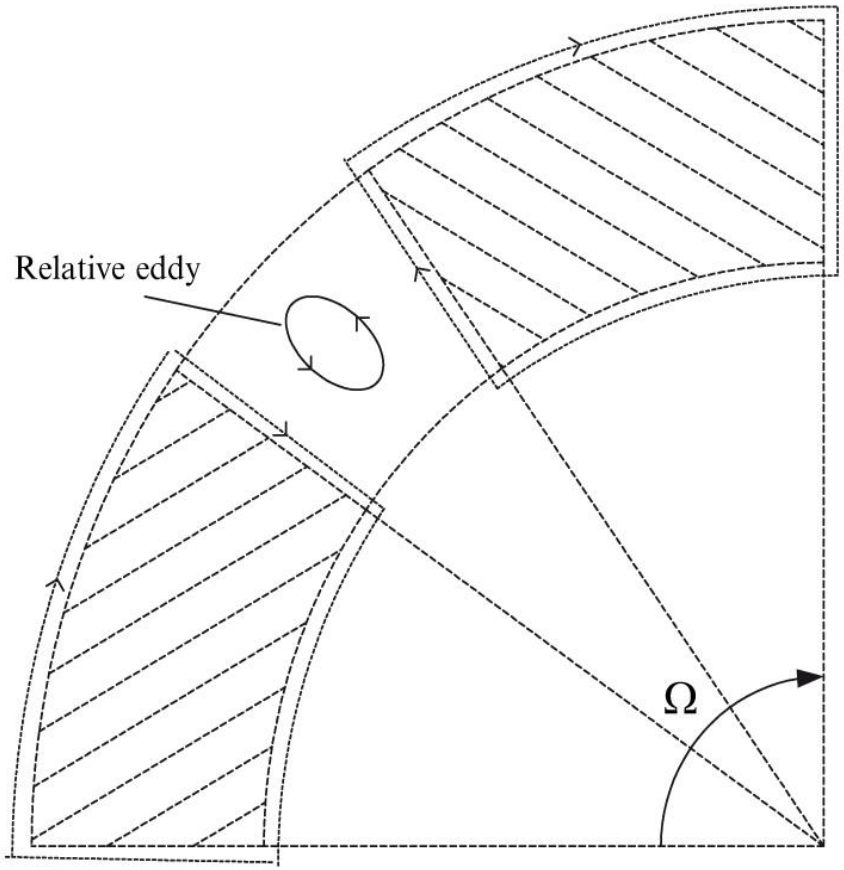

Fig. 4. The relative eddy in the PM channel.

The Actual Radial Channel

The actual characteristics of a hydraulic machine differ from the ideal case owing to two reasons: (i) the uneven spatial distribution of velocities in the blade passages, and (ii) the leakage and recirculation of flow and hydraulic losses such as friction and shock losses. These are completely different issues and shall be dealt with separately.

Slip factor

As a result of the unbalanced velocity distribution of the leading and trailing edges of a PM channel and the rotation effects [232], there exists, according to Stodola [198, 232], a *relative eddy* within the blade passage shown in Fig. 8.4. This results in the reduction of the tangential velocity components and is called *slip*, which is usually accounted for using a *slip factor*. For approximately radial blades, the *Stanitz* slip factor k_s ($80^o < \beta_2 < 90^o$) is

$$k_s = 1 - 0.63\pi/n_b \qquad (23)$$

where β_2 is the blade angle at exit and n_b is the number of the blades. When applying a slip factor, the pressure relation (8.22) becomes

$$\Delta p = \rho\Omega^2(k_s R_{out}^2 - R_{in}^2) + \frac{\rho}{2}(\frac{1}{A_1^2} - \frac{1}{A_2^2})Q^2 \qquad 24)$$

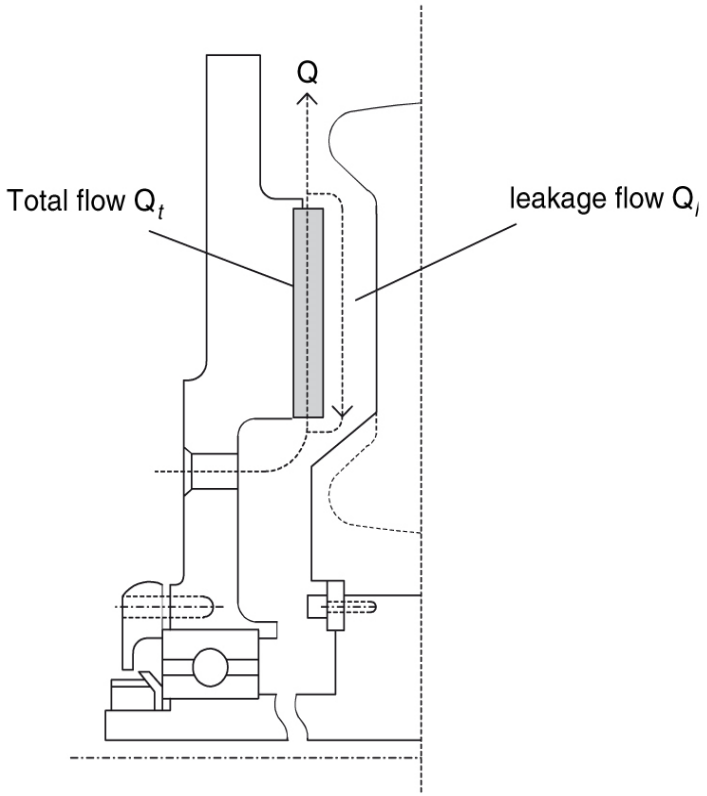

Fig. 5. Leakage flow in an AFPM machine (not to scale).

Shock, leakage and friction

Energy losses due to friction, separation of the boundary layer (shock loss) and leakage should also be considered in the flow analysis. As illustrated in Fig. 5, if the total volumetric flow rate through the PM channel is Q_t, the pressure difference between the PM exit and the entrance will cause a *leakage* or recirculation of a volume of fluid Q_l, thus reducing the flow rate at outlet to $Q = Q_t - Q_l$. The Q_l is a function of mass flow rate and discharge and leakage path resistances. The leakage flow reaches its maximum when the main outlet flow is shut.

These losses can be accounted for by introducing a pressure loss term Δp_l in eqn as follows

$$\Delta p = \rho\Omega^2(k_s R_{out}^2 - R_{in}^2) + \frac{\rho}{2}(\frac{1}{A_1^2} - \frac{1}{A_2^2})Q^2 - \Delta p_l \qquad .25)$$

System losses

As the air passes through the AFPM machine, the system pressure loss due to friction must be taken into account. The sum of these losses is given by:

$$\Delta p_{fr} = \frac{\rho Q^2}{2} \sum_{i=1}^{n} \frac{k_i}{A_i^2} \qquad .26)$$

where k_i and A_i are the loss coefficient and the cross section area of the flow path i respectively.

There are a number of sections through which the air flows in the AFPM machine (see Fig. .6). They are:

(1) entry into the rotor air inlet holes;
(2) passage through rotation short tube;
(3) bending of air from pipe to annulus (90°);
(4) round bend air passage (90°);
(5) contraction of air in the tapering passage;
(6) bending of air through the 90° elbow;
(7) entry to the permanent magnet channels;
(8) expansion of air through the tapering enlargement;
(9) abrupt expansion of the air on the exit of the channel;
(10) expansion as the air leaves the opening of the parallel rotor discs.

The loss coefficients associated with each section in eqn 26) are given in [61, 188, 198]. When the section is not circular, use is made of the hydraulic diameter to characterise the cross section. The hydraulic diameter is defined as $D_h = 4A/\wp$ where A is the cross-sectional area of the flow path and $\wp$ is the wetted perimeter.

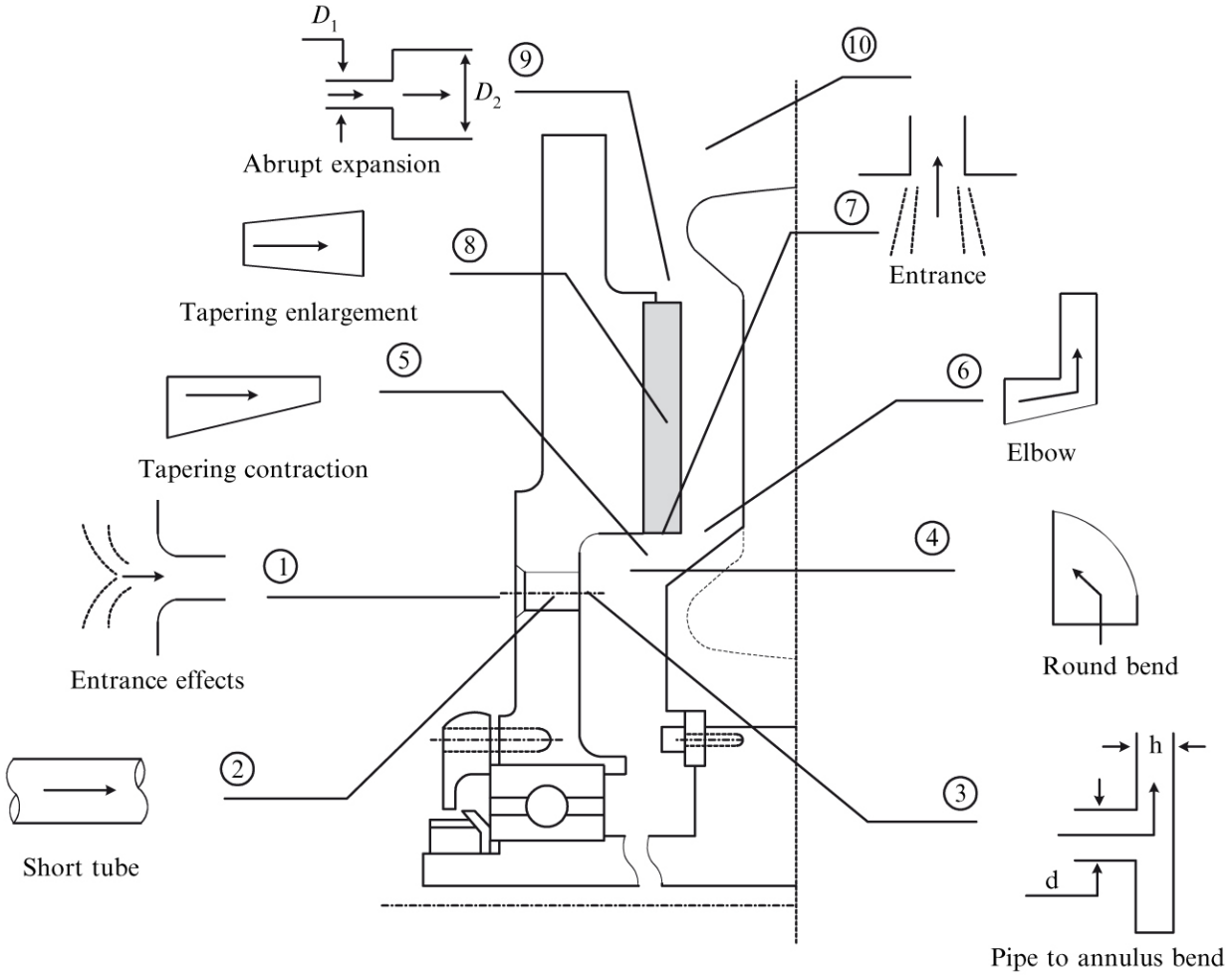

Fig. 6. System losses of an AFPM machine.

The loss coefficient for a pipe is given by $\lambda L/d$ where λ is a friction factor obtained as a function of Reynolds number Re and surface roughness from a *Moody diagram* [190]. To facilitate numeric calculations, the Moody diagram may be represented by [61]:

$$\begin{cases} \lambda &= 8\{(8/Re)^{12} + (X+Y)^{-\frac{3}{2}}\}^{\frac{1}{12}} \\ X &= \{2.457\ \ln\{(7/Re)^{0.9} + 0.27\gamma/D\}^{-1}\}^{16} \\ Y &= \{37530/Re\}^{16} \end{cases} \quad (27)$$

where $Re = \frac{\rho D_h Q}{\mu A}$ and where γ is the equivalent sand grain roughness [61].

Characteristics

It is now possible to relate the theoretical prediction obtained from the ideal flow model to the actual characteristic by accounting for the various losses discussed above.

Assuming that the AFPM machine (shown in Fig. 1) operates at a constant speed of 1200 rpm, the ideal developed pressure characteristic for a radial channel is a function described by eqn as shown in Fig. 6. After introducing the slip factor, the resultant curve is shown as a dotted line as

eqn (24). It was not possible to obtain a suitable correlation in the literature [248] for the pressure loss due to shock and leakage as was the case for the slip.

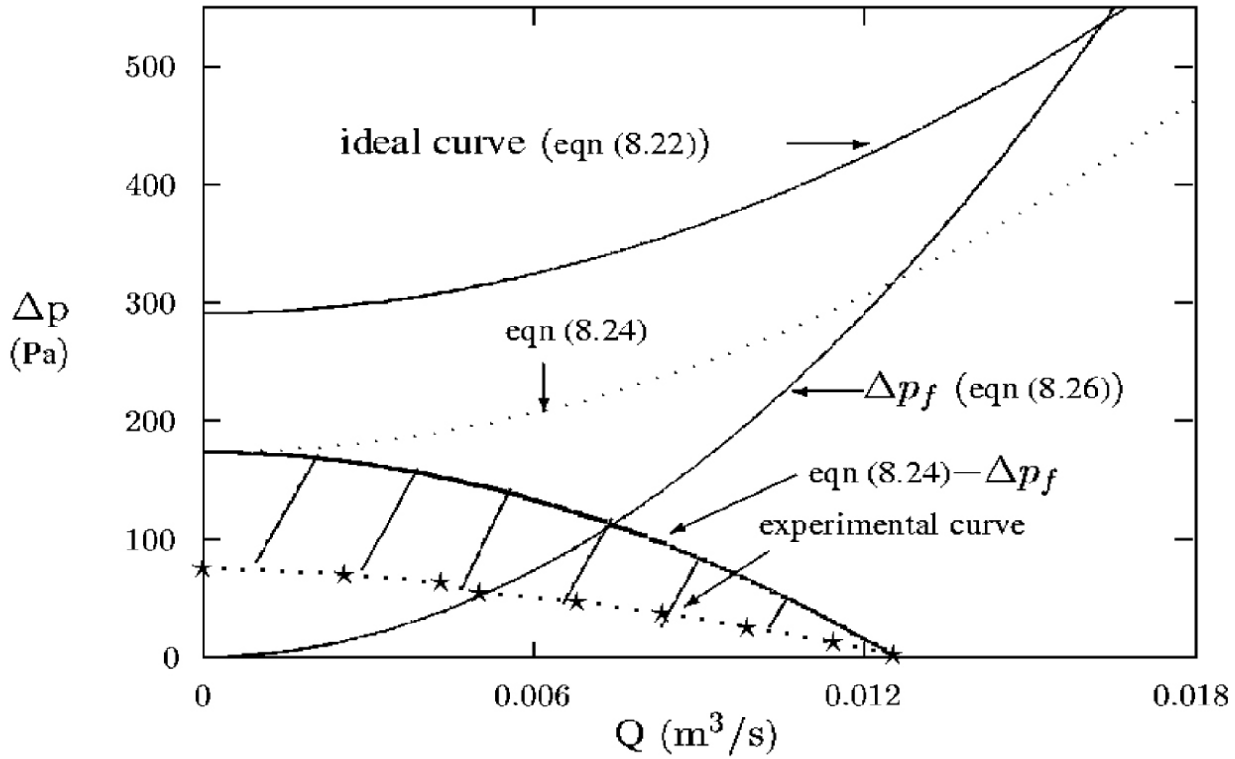

Fig. 7. Losses and characteristic curves at 1200 rpm.

The calculated characteristic curve without considering shock and leakage losses, i.e. eqn .24)–Δp_{fr} shown in Fig. .7, is significantly higher than the experimental one. The shaded area in Fig. 7 represents the shock and leakage losses. It can be seen that at low flow rates the shock and leakage losses are greater but tend to zero at the maximum flow rate. This has been discussed and experimentally validated in [260].

The derived characteristics describes the pressure relations of a single rotating PM disc facing a stator. For a double-sided AFPM machine with two identical coaxial rotating discs (Fig. .2) operating on the same stator, the characteristic curve presented in Fig. 7 represents only half of the AFPM machine. The characteristic curve of the whole machine may be obtained by adding flow rate at the same pressure, which is similar to two identical fans in parallel.

Flow and Pressure Measurements

Due to the nature and complexity of thermofluid analysis, the form of the system characteristics curve can at best be established by test. Depending on the machine topologies and size, the measurements may be taken either

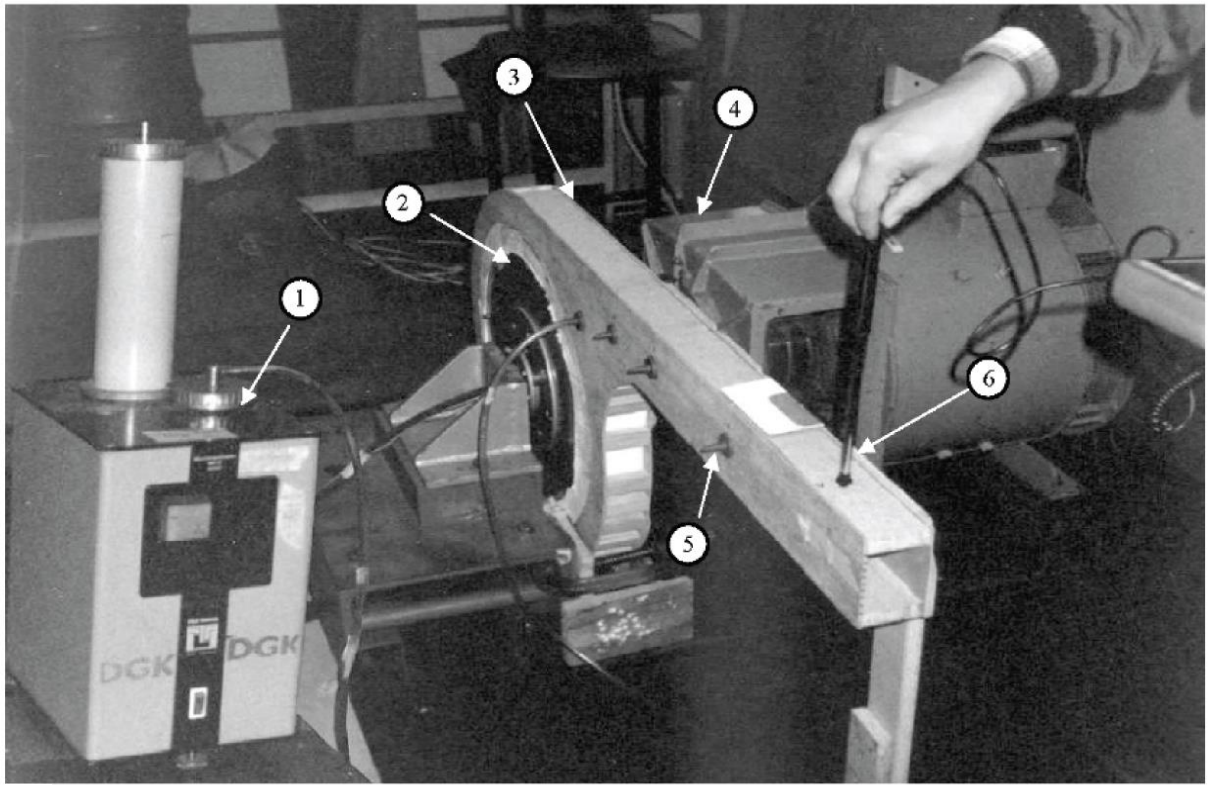

Fig. 8. The experimental set up. 1 — manometer, 2 — AFPM machine, 3 — discharge duct, 4 — prime mover (drive machine), 5 — pressure tapping point, 6 — wind speed probe. Photo courtesy of the *University of Stellenbosch*, South Africa.

To vary the flow rate, the test duct was fitted at its outer end with an obstruction. The test was started with no obstruction at the end of the discharge duct. The only resistance was then the duct friction, which was small and could be readily computed out of results. As the end of the duct was obstructed progressively, the flow was reduced and the static pressure increased to a maximum at zero volumetric flow rate. The static pressure difference Δp is measured as a function of volumetric flow rate $Q = A \times v$ for different motor speeds, where v is the linear speed.

The air flow-rate measurement can also be carried out by measuring inlet air pressure difference Δp, which is then used for calculating mass flow-rate $\dot{m}$ according to the following equation:

$$\dot{m} = \sqrt{2\rho\Delta p}\ A_d \qquad 28)$$

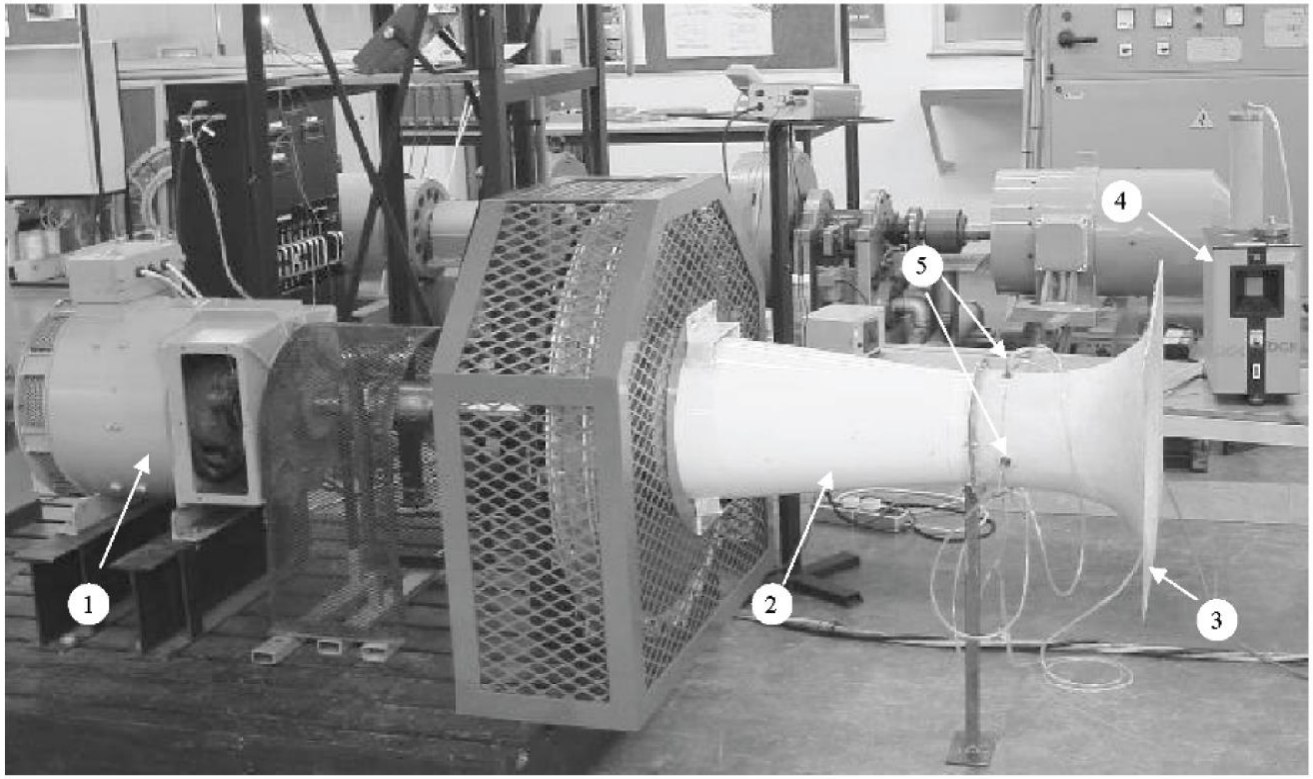

Fig. 9. Flow measurement at the air intake of AFPM machine. 1 — Prime mover (drive machine), 2 — inlet duct, 3 — bell mouth, 4 — manometer, and 5 — pressure tapping point. Photo courtesy of the *University of Stellenbosch*, South Africa.

where A_d is the cross section area of the inlet duct. Fig. 9 shows the setup of the flow measurement. A specially designed inlet duct with a bell mouth was mounted to the inlet (hub) of the AFPM machine. A few tapping points were made on the inlet duct for pressure measurements. The pressure drop through the bell mouth and inlet duct may often be assumed negligible.

3.2 AFPM Machines With External Ventilation

For medium to large power AFPM machines, the loss per unit heat dissipation area increases almost linearly with the power ratings. Thus the forced-cooling with the aid of external devices may be necessary. Some common techniques are described as follows.

External Fans

Large AFPM machines may require a substantial amount of air flow per unit time in order to bring out the heat generated in the stator windings. Depending on the operation conditions obtained on site, either an air-blast or a suction fan may be used as shown in Fig. 10. In both cases, intake and/or discharge ducts are needed to direct and condition the air flow. Since the inlet air temperature, for a given volumetric flow rate, has a significant effect on the machine temperature, this cooling arrangement can also help prevent recirculation of hot air should the machine operate in a confined space (e.g. small machine room). For high speed AFPM machines, a shaft-integral fan may be

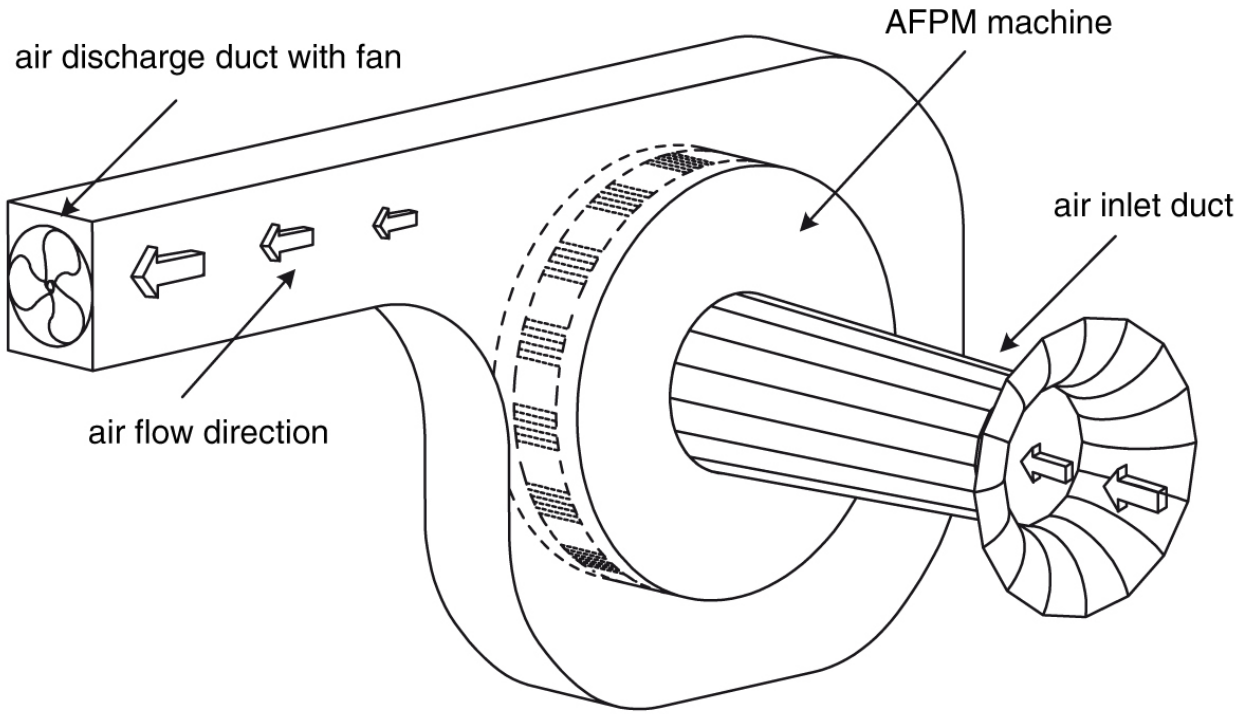

Fig. 10. AFPM machine with external air cooling.

a good option. Fig. .11 shows the assembly of a large power AFPM machine developed in the Department of Electrical and Electronic Engineering at the University of Stellenbosch, South Africa, in which the rotor hub part serves as both cooling fan and supporting structure for the rotor discs. It can be seen that the "blades" of the hub are not curved as the machine may operate in both directions of rotation.

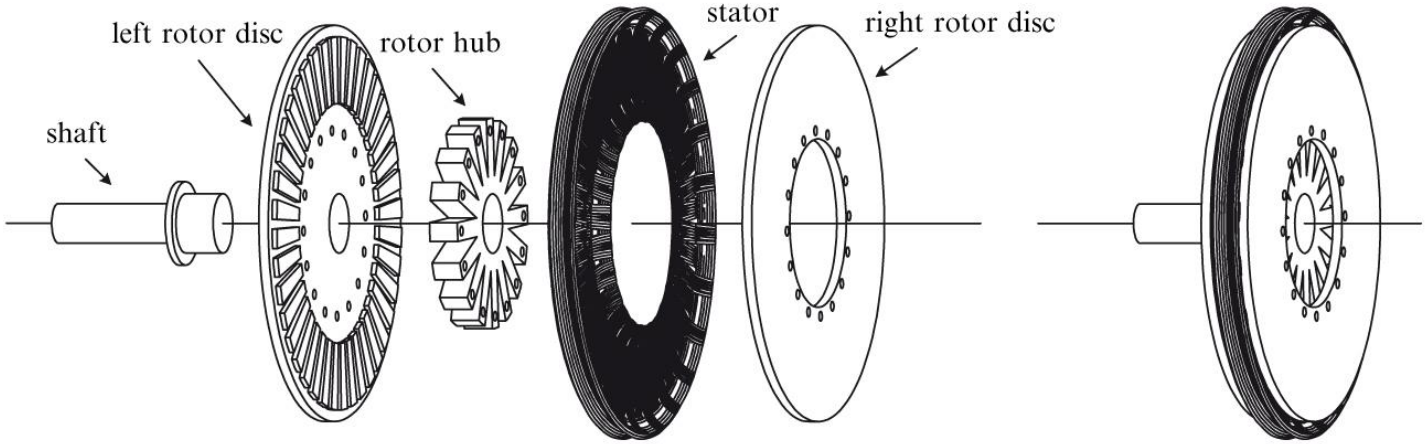

Fig. Configuration of the AFPM machine with shaft-integral fan.

Heat Pipes

The concept of a passive two-phase heat transfer device capable of transferring large amount of heat with a minimal temperature drop was introduced by R.S.

Gaugler of the General Motors Corporation in 1942. This device received little attention until 1964, when Grover and his colleagues at Los Alamos National Laboratory, NM, U.S.A., published the results of an independent investigation and first used the term *heat pipe*. Since then, heat pipes have been employed in many applications ranging from temperature control of the permafrost layer under the Alaska pipeline to the thermal control of optical surfaces in spacecraft.

A typical *heat pipe* consists of a sealed container with wicking material. The container is evacuated and filled with just enough liquid to fully saturate the wick. A heat pipe has three different regions, namely (i) *an evaporator* or heat addition region of the container, (ii) *a condenser* or heat rejection region, and (iii) *an adiabatic* or isothermal region. If the evaporator region is exposed to a high temperature, heat is added and the working fluid in the wicking structure is heated until it evaporates. The high temperature and the corresponding high pressure in this region cause the vapour to flow to the cooler condenser region, where the vapour condenses, dissipating its latent heat of vaporisation. The capillary forces existing in the wicking structure then pump the liquid back to the evaporator. The wick structure thus ensures that the heat pipe can transfer heat whether the heat source is below the cooled end or above the cooled end.

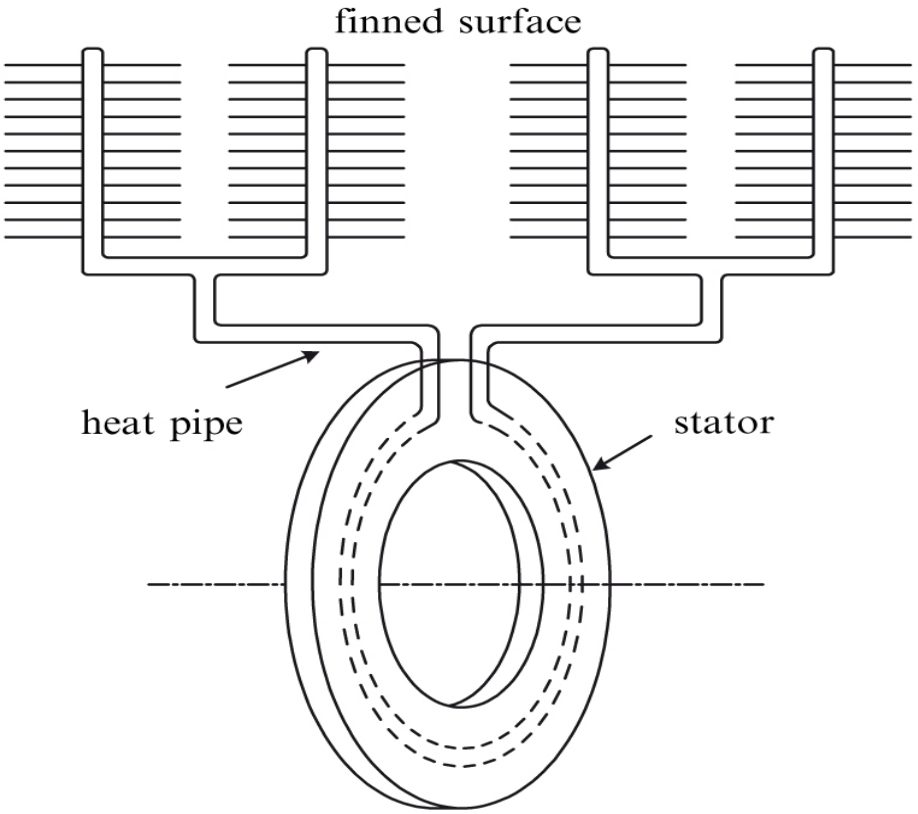

Fig. 12. AFPM machine cooled by heat pipes.

A heat pipe presents an alternative means for removing the heat from the AFPM machine. The heat pipe in an AFPM machine may be configured as shown in Fig. 12. Heat is transferred into the atmosphere through the finned

surface. The finned surface is cooled by air moving over the fins. The heat loss removed by the heat pipe, ΔP_{hp}, is given by [235]:

$$\Delta P_{hp} = \frac{\vartheta_{hot} - \vartheta_{cold}}{\frac{1}{h_{hot} A_{hot}} + \frac{1}{h_{cold} A_{cold}} + \frac{1}{\eta_{fin} h_{fin} A_{fin}}} \quad .29)$$

where ϑ_{hot} is the average temperature of the elements that surround the heat pipe in the stator, ϑ_{cold} is the average temperature of the air cooling the finned surface, h_{hot} is the convective heat transfer coefficient on the inside wall of the heat pipe in the stator, A_{hot} is the exposed area of the heat pipe in the stator, h_{cold} is the convection heat transfer coefficient on the inside wall of the heat pipe in the finned area, A_{cold} is the exposed area of the heat pipe at the finned surface, η_{fin} is the efficiency of the finned surface, h_{fin} is the convection heat transfer coefficient on the surface of the fins and A_{fin} is the total exposed area of the finned surface.

The heat removed through cooling pipes can be calculated by using eqn 29). However, the heat transfer coefficients, h_{hot} and h_{cold}, are calculated using the following relationships:

(i) for laminar flow, i.e. $\mathrm{Re}_d = \frac{\rho v d}{\mu} < 2000$, where v is the flow velocity and d is the diameter of the water pipe, the Nusselt number may be obtained using following empirical relation [124]

$$Nu_d = 1.86(Re_d Pr)^{\frac{1}{3}}(\frac{d}{L_p})^{\frac{1}{3}}(\frac{\mu}{\mu_w})^{0.14} \quad 30)$$

where L_p is the length of the water pipe, μ and μ_w are the dynamic viscosity of water at inlet and wall temperature respectively.

(ii) for turbulent flow, i.e. $\mathrm{Re}_d = \frac{\rho v d}{\mu} > 2000$, the Nusselt number may be calculated as [134]

$$Nu_d = 0.023 {Re_d}^{0.8} Pr^n \quad 31)$$

where

The heat removed through cooling pipes can be calculated by using eqn (8.29). However, the heat transfer coefficients, h_{hot} and h_{cold}, are calculated using the following relationships:

(i) for laminar flow, i.e. $\mathrm{Re}_d = \frac{\rho v d}{\mu} < 2000$, where v is the flow velocity and d is the diameter of the water pipe, the Nusselt number may be obtained using following empirical relation [124]

$$Nu_d = 1.86(Re_d Pr)^{\frac{1}{3}}(\frac{d}{L_p})^{\frac{1}{3}}(\frac{\mu}{\mu_w})^{0.14}$$

where L_p is the length of the water pipe, μ and μ_w are the dynamic viscosity of water at inlet and wall temperature respectively.

(ii) for turbulent flow, i.e. $\mathrm{Re}_d = \frac{\rho v d}{\mu} > 2000$, the Nusselt number may be calculated as [134]

$$Nu_d = 0.023 {Re_d}^{0.8} Pr^n \qquad 31)$$

where

$$n = \begin{cases} 0.4 & \text{for heating of the water,} \\ 0.3 & \text{for cooling of the water.} \end{cases}$$

4 Lumped Parameter Thermal Model

Lumped-parameter circuits, consisting of a network of thermal resistances, thermal capacitances, nodal temperatures and heat sources, have been used extensively to represent the complex distributed thermal parameters of electrical machines [84, 159, 245].

4.1 Thermal Equivalent Circuit

A *thermal equivalent circuit* is essentially an analogy of an electrical circuit, in which the heat (analogous to *current*) flowing in each path of the circuit is given by a temperature difference (analogous to *voltage*) divided by a thermal resistance (analogous to *electrical resistance*). For conduction, the thermal resistance depends on the thermal conductivity of the material, k, and the length, l, and cross-sectional area, A_d, of the heat flow path and may be expressed as

$$R_d = \frac{l}{A_d k} \qquad .32)$$

Thermal resistances for convection is defined as:

$$R_c = \frac{1}{A_c h} \tag{33}$$

where A_c is the surface area of convective heat transfer between two regions and h is the convection coefficient.

The thermal resistance for radiation between two surfaces is

$$R_r = \frac{\frac{1-\varepsilon_1}{\varepsilon_1 A_1} + \frac{1}{A_1 F_{12}} + \frac{1-\varepsilon_2}{\varepsilon_2 A_2}}{\sigma[(\vartheta_1 + 273) + (\vartheta_2 + 273)][(\vartheta_1 + 273)^2 + (\vartheta_2 + 273)^2]} \tag{34}$$

It is seen that the radiation thermal resistance in eqn 34) depends on the difference of the third power of the temperature, the surface spectral property ε and the surface orientation taken into account by a form factor F.

The thermal circuit in the steady state consists of thermal resistances and heat sources connected between motor component nodes. For transient analysis, the thermal capacitances are used additionally to account for the change of internal energy in the various parts of the machine with time. The heat capacitance is defined as:

$$C = \rho V c_v = m c_v \qquad 35)$$

where c_v is the heat capacity of the material, ρ is the density, and V and m are the volume and mass of the material respectively. Fig. 13a shows a sectional view of an AFPM machine with a coreless stator. It can be observed that the AFPM stator is symmetrical from a heat transfer perspective and each half of the machine from the centre line mirrors the other half. It is therefore reasonable to model only half of the machine as shown in Fig. 13b.

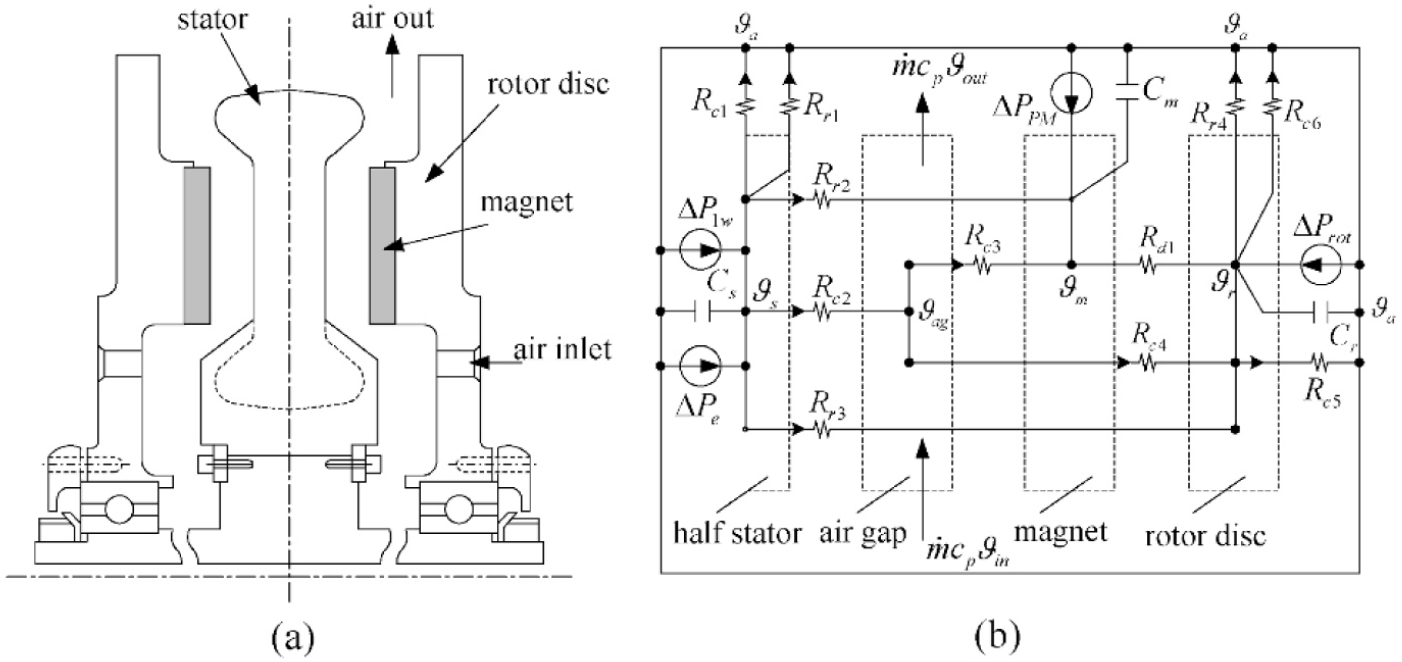

Fig. 13. The thermal resistance circuit of an AFPM brushless machine with coreless stator.

The heat source terms ΔP_{1w}, ΔP_e, ΔP_{PM} and ΔP_{rot} stand for winding losses (2.49), eddy current losses in one half of the stator winding (2.68), losses in PMs (2.61) and rotational losses (2.70) per one rotor disc respectively. C_s, C_m and C_r are the thermal capacitances of stator, PMs and rotor steel disc respectively. The heat resistances used in the circuit are described in Table 8.3.

In the lumped parameter thermal circuit analysis, it is often assumed that the temperature gradients within certain part of the machine is negligible. This assumption can only be made if the internal resistance to heat transfer is small compared with the external resistance [124]. The *Biot number*, B_i, is often used for determining the validity of this assumption. In the case that internal conduction resistance is compared with external convection resistance, B_i is defined as:

$$B_i = \frac{\bar{h}_c L}{k_s} \qquad (36)$$

where k_s is the thermal conductivity of the solid material, L is the characteristic length of a solid body and $\bar{h}_c$ is the convection heat transfer coefficient. The criterion $B_i < 0.1$ ensures that the internal temperature will not differ

Table 3. Definition of thermal resistances

Symbols	Definition
R_{c1}	Convection resistance from stator end-winding to open air
R_{c2}	Convection resistance from stator to air-gap
R_{c3}	Convection resistance from air-gap to permanent magnets
R_{c4}	Convection resistance from air-gap to rotor disc plate
R_{c5}	Convection resistance from rotor disc to open air
R_{c6}	Convection resistance from rotor radial periphery to open air
R_{r1}	Radiation resistance from stator end-winding to environment
R_{r2}	Radiation resistance from stator to permanent magnets
R_{r3}	Radiation resistance from stator to rotor disc
R_{r4}	Radiation resistance from rotor radial periphery to environment
R_{d1}	Conduction resistance from PMs to rotor disc

from that at the surface of a solid body by more than 5% [190], and thus is frequently used.

4.2 Conservation of Energy

If conservation of energy is applied, the rate of internal energy change in each part of a machine (also called *control volume*) may be written as follows:

$$\frac{\Delta U}{\Delta t} = C\frac{\Delta \vartheta}{\Delta t} = \Delta P_{in} - \Delta P_{out} + \dot{m}_{in} i_{in} - \dot{m}_{out} i_{out} \qquad 37)$$

where U is the internal energy, $\dot{m}$ is the mass flow rate and i is the *enthalpy* and C is the thermal capacitance of a control volume.

For steady-state conditions, $\frac{\Delta U}{\Delta t} = 0$ and therefore,

$$0 = \Delta P_{in} - \Delta P_{out} + \dot{m}_{in} i_{in} - \dot{m}_{out} i_{out} \qquad 38)$$

These equations are applied to each part (the stator, air gap, PM and rotor disc) of the AFPM machine to obtain a set of equations with the temperatures of the parts being the only unknowns. This set of equations is rather complex but is readily solved using for example, the *Gauss-Seidel* iteration. It should be noted that the term $(\dot{m}_{in} i_{in} - \dot{m}_{out} i_{out})$ in the above equations represents internal heat removed due to the air flow pumped through the machine. This air flow is of paramount importance to the cooling of the machine. The determination of the air gap temperature in the thermal equivalent circuit is only possible if the mass flow rate through the air gap can be somehow predicted, hence the necessity of using the fluid-flow model described in section 3.1.

5 Machine Duties

Depending on the load conditions, there are mainly three types of duties or operation modes for all the electrical machines, i.e. continuous duty, short-time duty and intermittent duty.

5.1 Continuous Duty

When an electrical machine operates for a long period so that the temperatures of various parts of the machine reach steady-state at a given ambient temperature, this operation mode is called *continuous duty*. Due to the different physical properties, the final stablised temperatures in various parts of the machine may vary greatly. The machine can be continuously operated for an infinitely long time without exceeding the temperature limits specified for each component of the machine. When only the solid parts of the machine are considered, the air flow term in the eqn (8.37) is ignored. The temperature rise versus time relationship in a control volume of the machine may be derived based on the theory of solid body heating as [159]:

$$\vartheta_c = \Delta P \; R(1 - e^{-\frac{t}{\tau}}) + \vartheta_o \; e^{-\frac{t}{\tau}} \tag{39}$$

where R is the thermal resistance, $\tau = RC$ is the thermal time constant, C is the thermal capacitance , ΔP is the heat loss flow, and ϑ_o is the initial temperature rise of the control volume . In a case where $\vartheta_o = 0$, the above equation is simply:

$$\vartheta_c = \Delta P \; R(1 - e^{-\frac{t}{\tau}}) \tag{40}$$

According to the properties of an exponential function, the final temperature rise $\vartheta_{cf} = \Delta P \times R$. Fig. 8.14a shows the typical transient temperature response of an AFPM machine operated continuously.

.5.2 Short-Time Duty

Short-time duty means that machine operates only within a short specified period followed by a long period of rest or no-load condition. The operation time is so short that the machine does not attain its steady-state temperature, and the machine practically returns to its cold state after a long period of rest. Given the operation time t_s, the temperature rise of the machine can be found by using eqn .40) as

$$\vartheta_s = \Delta P\ R(1 - e^{-\frac{t_s}{\tau}}) = \vartheta_{cf}\ (1 - e^{-\frac{t_s}{\tau}}) \qquad 41)$$

Compared with continuous duty, it is obvious that $\vartheta_s < \vartheta_{cf}$. This implies that the permissible load for the same machine in short time duty can be $1/(1 - e^{-\frac{t_s}{\tau}})$ times greater than that in continuous duty. Fig. 14b shows the typical temperature rise curve for short time duty machines.

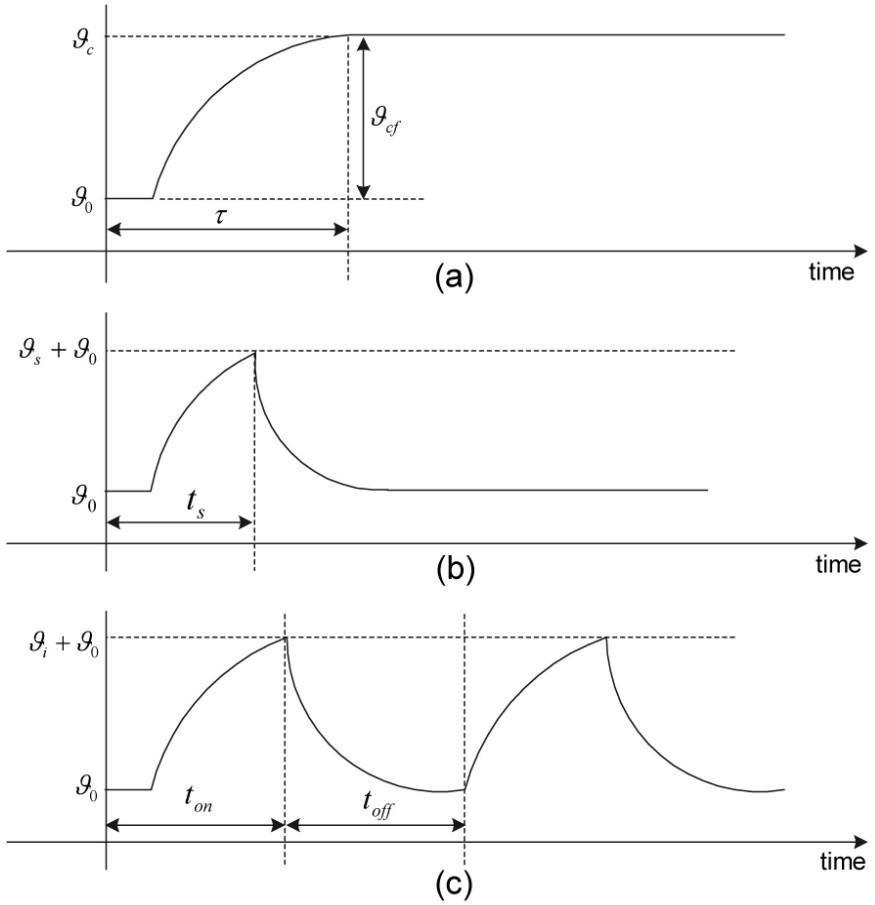

Fig. 14. Characteristic temperature curves of AFPM machines for different operation modes: (a) continuous duty, (b) short-time duty, (c) intermittent duty.

5.3 Intermittent Duty

The *intermittent duty* is characterised by short-time operations alternated with short-time pause intervals. Suppose a machine operates for a short period of t_{on} and then stops for a period of t_{off}, the cycle t_{cy} is then $t_{cy} = t_{on} + t_{off}$. The duty cycle d_{cy} may be defined as:

$$d_{cy} = \frac{t_{on}}{t_{on} + t_{off}} \tag{42}$$

The temperature rise of the machine ϑ_i during the t_{on} period can be calculated by using eqn 39) provided that thermal time constant and the steady-state temperature rise for continuous operation duty are known. During the t_{off} period, the machine loss $\Delta P = 0$ and the machine's temperature decreases according to an exponential function, i.e. $\vartheta_i e^{-t_{off}/\tau}$ before the second cycle sets in.

After many subsequent cycles, the machine's temperature variation becomes uniform and tends to be within a certain limited range (see Fig. 14c).

Under the same load and cooling condition, the maximum stablised temperature of a machine in intermittent operation duty is smaller than that in continuous duty. Hence, similar to short-time operation duty, a machine operated in intermittent duty has overload capacity.

Numerical Example 1

A self-cooled 8-pole, 16-kW AFPM generator with an ironless stator as shown in Fig .2 will be considered. The outer diameter is $D_{out} = 0.4$ m and the inner diameter is $D_{in} = 0.23$ m. The magnet width–to–pole pitch ratio $\alpha_i = 0.8$ and thickness of a rotor disc $d = 0.014$ m. The measured flow characteristic curves are shown in Fig. 15. At rated speed 1260 rpm, the total losses are 1569 W, of which (i) rotational losses $\Delta P_{rot} = 106$ W; (ii) eddy current losses in the stator $\Delta P_e = 23$ W; (iii) stator winding losses (rated) $\Delta P_{1w} = 1440$ W.

Find:

(a) Convective heat transfer coefficients of the disc system

(b) Steady-state temperatures at different parts of the machine.

Solution

(a) Convective heat transfer coefficients of the disc system

The dynamic viscosity, density and thermal conductivity of air are assumed to be $\mu = 1.8467 \times 10^{-5}$ Pa s, $\rho = 1.177$ kg/m^3 and $k = 0.02624$ W/(m °C) respectively in the following convective coefficients calculations.

Convection coefficient: outside rotor disc surface

At rated speed, the Reynolds number

$$Re = \rho \frac{\Omega D_{out}^2}{4\mu} = 1.177 \times \frac{2\pi \times 1260/60 \times 0.4^2}{4 \times 1.846 \times 10^{-5}} = 336384.7$$

the transition between laminar and turbulent flow takes place at

$$r_c = \sqrt{\frac{2.5 \times 10^5 \nu}{\Omega}} = \sqrt{\frac{2.5 \times 10^5 \times 1.569 \times 10^{-5}}{2\pi \times 1260/60}} = 0.172 < \frac{D_{out}}{2} \text{ m}$$

The average Nusselt number of the disc

$$\overline{Nu} = 0.015 \times Re^{\frac{4}{5}} - 100 \times (\frac{2r_c}{D_{out}})^2$$

$$= 0.015 \times 336384.7^{\frac{4}{5}} - 100 \times \left(\frac{2 \times 0.172}{0.4}\right)^2 = 321.9$$

The average heat transfer coefficient at the outer surface of the disc

$$\overline{h}_{fr} = \frac{k}{D_{out}/2} \times \overline{Nu} = \frac{0.02624}{0.4/2} \times 321.9 = 42.2 \text{ W/(m}^2 \text{ }^{\circ}\text{C)}$$

Convection coefficient: rotor disc peripheral edge

The Prandtl number is taken as $Pr = 0.7$ (Atmospheric pressure, 25 °C). The Reynolds number at disc periphery

$$Re_D = \Omega \frac{D_{out}^2}{\nu} = \frac{2\pi \times 1260}{60} \frac{0.4^2}{1.569 \times 10^{-5}} = 1345538.8$$

The average Nusselt number is

$$\overline{Nu} = 0.133 \times {Re_D}^{\frac{2}{3}} \times Pr^{\frac{1}{3}} = 0.133 \times 1345538.8^{\frac{2}{3}} \times 0.7^{\frac{1}{3}} = 1439.3$$

The average heat transfer coefficient around the radial periphery

$$\overline{h}_p = \frac{k}{D_{out}} \times \overline{Nu} = \frac{0.02624}{0.4} \times 1439.3 = 94.4 \text{ W/(m}^2 \text{ °C)}$$

Convection coefficient: rotor-stator system

The volumetric flow rate of the machine at rated speed can be looked up from Fig. 15. Assuming equal flow on both sides of stator, the equivalent flow rate is taken as $Q = 0.013$ m^3/s. The average Nusselt number

$$\overline{Nu} = 0.333\frac{Q}{\pi\nu(D_{out}/2)} = 0.333 \times \frac{0.013}{\pi 1.566 \times 10^{-5} \times (0.4/2)} = 440$$

The average heat transfer coefficient between two discs

$$\overline{h}_{rs} = \frac{2k}{D_{out}} \times \overline{Nu} = \frac{2 \times 0.02624}{0.4} \times 440 = 57.7 \text{ W/(m}^2\ ^{\circ}\text{C)}$$

(b) Steady-state temperatures at different parts of the machine

If the radiation from the rotor disc to ambient, the convection from the stator overhang to air flow, and the conduction resistance between magnets and rotor are ignored, the generic thermal equivalent circuit given in Fig. 13 is simplified as shown in Fig. 16.

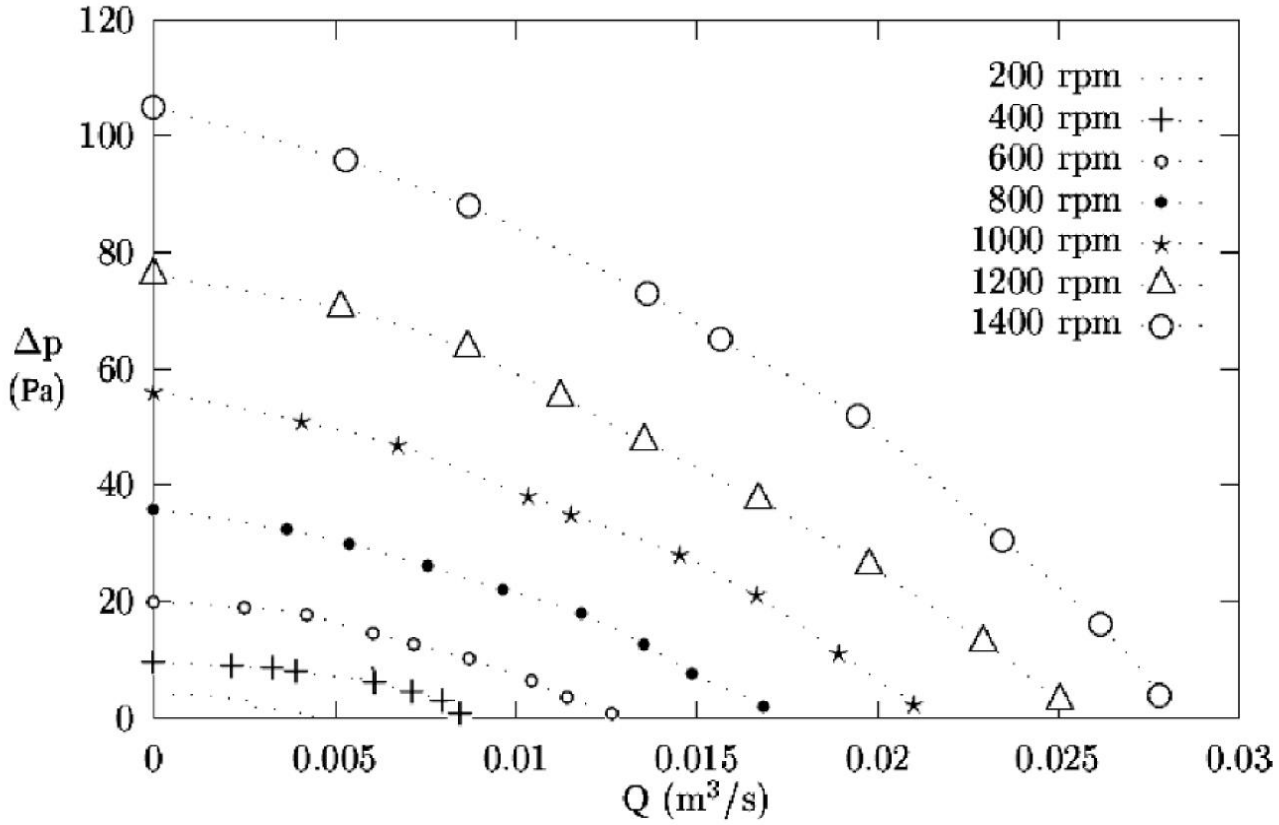

Fig. 15. Measured characteristic curves of the AFPM machine. *Numerical example 8.1*.

Control volume 1 (*half of the stator*)

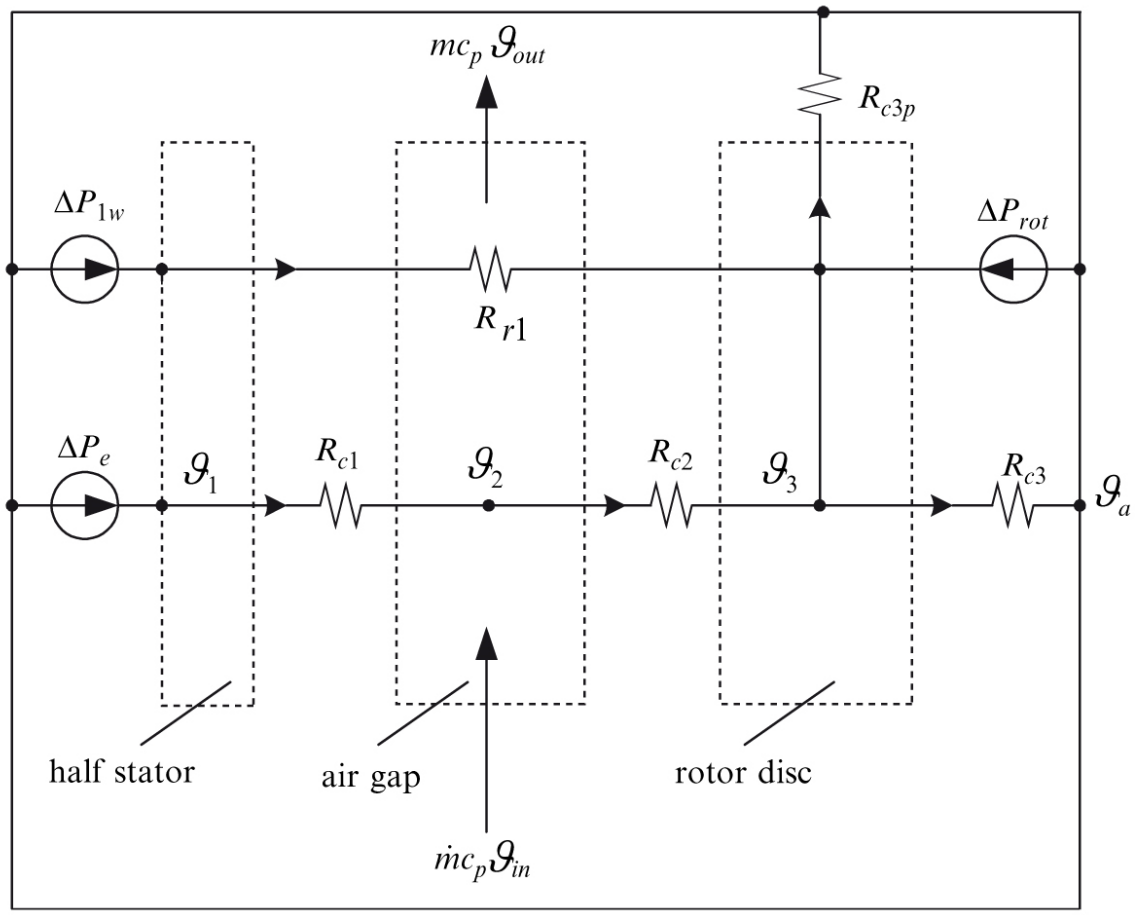

Fig. 16. Simplified thermal equivalent circuit. *Numerical example 8.1.*

The convection heat transfer resistance between the stator and air flow in the air gap is

$$R_{c1} = \frac{1}{\overline{h}_{rs} \times \frac{\pi}{4}(D_{out}^2 - D_{in}^2)} = \frac{1}{57.7 \times \frac{\pi}{4}(0.4^2 - 0.23^2)} = 0.223 \ ^{\circ}\text{C/W}$$

The radiation heat transfer resistance between the stator and rotor discs is

$$R_{r1} = \frac{\frac{1-\varepsilon_1}{\varepsilon_1 A_1} + \frac{1}{A_1 F_{12}} + \frac{1-\varepsilon_2}{\varepsilon_2 A_2}}{\sigma[(\vartheta_1 + 273) + (\vartheta_2 + 273)][(\vartheta_1 + 273)^2 + (\vartheta_2 + 273)^2]}$$

in which the areas of both discs can be taken as the same, i.e. $A_1 = A_2 = \frac{\pi}{4}(D_{out}^2 - D_{in}^2) = 0.084$ m^2, the shape factor $F_{12} = 1$, the *Stefan-Boltzmann* constant $\sigma = 5.67 \times 10^{-8}$ W/(m^2 K^4), the emissivity of epoxy encapsulated stator $\varepsilon_1 = 0.85$. Since part of the rotor disc is covered with PMs, the emissivity of the rotor disc is defined based on the proportion of different materials, i.e.

$$\varepsilon_2 = \varepsilon_{fe}\alpha_i + \varepsilon_{pm}(1 - \alpha_i) = 0.3 \times 0.8 + 0.9 \times (1 - 0.8) = 0.42$$

Apparently R_{r1} is a function of ϑ_1 and ϑ_2, an iterative approach has to be used to solve R_{r1} for different temperatures.
According to conservation of energy, the steady-state energy equation for *control volume 1* can be written as

$$\frac{1}{2}(\Delta P_{1w} + \Delta P_e) - \frac{\vartheta_1 - \vartheta_2}{R_{c1}} - \frac{\vartheta_1 - \vartheta_3}{R_{r1}} = 0 \qquad 43)$$

Control volume 2 (*air gap*)

The convection heat transfer resistance from air gap to the rotor disc may be taken as the same as that from stator to air gap, i.e. $R_{c2} = R_{c1}$. The mass flow rate $\dot{m} = \rho Q = 1.177 \times 0.013 = 0.0153$ kg. Assume that the air temperature at the machine inlet is ambient temperature, i.e. $\vartheta_{in} = \vartheta_a$ and the air gap average temperature $\vartheta_2 = \frac{1}{2}(\vartheta_{out} + \vartheta_{in})$. The heat dissipated due to the air flow is

$$\dot{m}_{out} i_{out} - \dot{m}_{in} i_{in} = \dot{m}\ c_p\ (\vartheta_{out} - \vartheta_{in}) = 2\dot{m}\ c_p\ (\vartheta_2 - \vartheta a)$$

$$= 2 \times 0.0153 \times 1005 \times (\vartheta_2 - 20)$$

The steady-state energy equation for *control volume 2* is

$$\frac{\vartheta_1 - \vartheta_2}{R_{c1}} - \frac{\vartheta_2 - \vartheta_3}{R_{c2}} - 2 \times 0.0153 \times 1005 \times (\vartheta_2 - 20) = 0 \qquad 14)$$

Control volume 3 (*rotor disc*)

The convection heat transfer resistance at the outside surface of the disc is

$$R_{c3} = \frac{4}{\overline{h}_{fr}\pi {D_{out}}^2} = \frac{4}{42.4 \times \pi \times 0.4^2} = 0.1877 \text{ °C/W}$$

The convection heat transfer resistance at the periphery of the disc is

$$R_{c3p} = \frac{1}{\overline{h}_p \ \pi \ D_{out} \ d} = \frac{1}{94.4 \times \pi \times 0.4 \times 0.014} = 0.602 \text{ °C/W}$$

The steady-state energy equation for *control volume 3* is

$$\frac{\vartheta_2 - \vartheta_3}{R_{c2}} + \frac{\vartheta_1 - \vartheta_3}{R_{r1}} + \frac{1}{2}\Delta P_{rot} - \frac{\vartheta_3 - \vartheta_a}{R_{c3}} - \frac{\vartheta_3 - \vartheta_a}{R_{c3p}} = 0 \qquad 45)$$

Having established the energy equations (43),(44) and (.45) for each part of the machine, the steady-state temperatures can be found by solving these equations. Due to the temperature dependency of R_{r1}, a simple computer program using *Gauss Seidel* iteration has been created to find the solutions of the equations. The results are given in Table .4.

Table 4. Predicted temperature rises

Machine parts	Temperature rise, °C
Stator winding, ϑ_1	114.9
Air-gap flow, ϑ_2	21.35
Rotor disc, ϑ_3	18.32

Numerical Example ˆ 2

A totally enclosed AFPM brushless machine has a power loss of ΔP_{1W} =2500 W in the stator winding at continuous duty. The machine's outer and inner diameters are $D_{out} = 0.72$ m and $D_{in} = 0.5$ m respectively. To remove the heat from the stator, use is made of heat pipes for direct cooling of the motor as shown in Fig. 12. The convection heat transfer coefficients on the inside wall of heat pipes in the stator and in the finned area are assumed to be $h = 1000$ W/(m^2 °C). The average convective heat transfer coefficient on the fin surface is taken as $h_{fin} = 50$ W/(m^2 °C). The finned surface has an overall area of $A_{fin} = 1.8$ m^2 and an efficiency of $\eta_{fin} = 92\%$. The length of heat pipe embedded in the finned surface is $l_{fin} = 1.5$ m. Find:

(a) Steady-state temperature of the stator winding if the heat pipe with a diameter $D_{hp} = 9$ mm is placed along the average radius of the stator

(b) Steady-state temperatures of the stator winding if the heat pipe is replaced by a $d = 9$ mm water cooling pipe, in which water (with an average temperature of 60°C) flows at $v_w = 0.5$ m/s.

Solution

(a) Steady-state temperature of the stator winding if the heat pipe with a diameter $D_{hp} = 9$ mm is placed along the average radius of the stator

Assuming the outside wall of the heat pipe is in full contact with the stator winding and finned surface, the exposed area of the heat pipe in the stator will be

$$A_{hot} = \pi D_{hp} \frac{\pi(D_{out} + D_{in})}{2} = 0.009\pi \times \frac{\pi(0.72 + 0.5)}{2} = 0.0542 \text{ m}^2$$

The exposed area of the heat pipe embedded in the finned surface will be

$$A_{cold} = \pi D_{hp} l_{fin} = 0.009\pi \times 1.5 = 0.0424 \text{ m}^2$$

Assuming the temperature of cooling air over the finned area to be $\vartheta_{cold} = 30^{\circ}\text{C}$, the steady-state temperature of the stator may be obtained by using eqn (8.29)

$$\vartheta_{stator} = \vartheta_{cold} + \Delta P_{hp}\left(\frac{1}{h_{hot}A_{hot}} + \frac{1}{h_{cold}A_{cold}} + \frac{1}{\eta_{fin}h_{fin}A_{fin}}\right)$$

$$= 30 + 2500\left(\frac{1}{1000 \times 0.0542} + \frac{1}{1000 \times 0.0424} + \frac{1}{0.92 \times 50 \times 1.8}\right) = 165.3\ ^{\circ}\text{C}$$

(b) Steady-state temperatures of the stator winding if the heat pipe is replaced by a water cooling pipe of diameter $d = 9$ mm, in which water flows at 0.5 m/s.

The Reynolds number is first calculated to determine the flow regime. The properties of water at 60°C are $\rho = 983.3$ kg/m^3, $c_p = 4179$ J/(kg °C), $\mu = 4.7\times10^{-4}$ Pa s, $k = 0.654$ W/(m °C), $Pr = \mu c_p/k = 4.7\times10^{-4}\times4179/0.654 = 3$, $Re_d = \rho v_w d/(2\mu) = 983.3 \times 0.5 \times 0.009/4.7 \times 10^{-4} = 9414.6 > 2000$, so that the flow is turbulent. Thus, the Nusselt number for the heating of the water is

$$Nu_{dh} = 0.023 Re_d^{0.8} Pr^{0.4} = 0.023 \times 9414.6^{0.8} \times 3^{0.4} = 53.9$$

while the Nusselt number for the cooling of the water is

$$Nu_{dh} = 0.023 Re_d^{0.8} Pr^{0.3} = 0.023 \times 9414.6^{0.8} \times 3^{0.3} = 48.3$$

The convection heat transfer coefficients of the water pipe inside the stator h_{hot} and in the finned area h_{cold} are calculated as

$$h_{hot} = \frac{k\ Nu_{dh}}{d} = \frac{0.654 \times 53.9}{0.009} = 3916.7\ W/(m^2\ ^oC)$$

$$h_{cold} = \frac{k\ Nu_{dc}}{d} = \frac{0.654 \times 48.3}{0.009} = 3509.8\ W/(m^2\ ^oC)$$

The steady-state temperature in the stator can be calculated as in (a) with the exception that the heat transfer coefficients are different

$$\vartheta_{stator} = \vartheta_{cold} + \Delta P_{hp}\left(\frac{1}{h_{hot}A_{hot}} + \frac{1}{h_{cold}A_{cold}} + \frac{1}{\eta_{fin}h_{fin}A_{fin}}\right)$$

$$= 30 + 2500 \times \left(\frac{1}{3916.7 \times 0.0542} + \frac{1}{3509.8 \times 0.0424} + \frac{1}{0.92 \times 50 \times 1.8}\right) = 88.8\,^oC$$


THANK YOU